Optimization of an active device for global control of low-frequency wall reflections in a semi-anechoic room

Emmanuel Friot, Cédric Pinhède, Philippe Herzog, Romain Boulandet

25-29 August 2024
inter.noise
NANTES FRANCE

Optimization of an active device for global control of low-frequency wall reflections in a semi-anechoic room

Emmanuel Friot [1]
Aix Marseille Univ, CNRS, Centrale Marseille, LMA UMR7031
Laboratoire de Mécanique et d'Acoustique
4 Impasse Nikola Tesla, CS 40006 13453 Marseille Cedex 13, France

Cédric Pinhède [2]
Aix Marseille Univ, CNRS, Centrale Marseille, LMA UMR7031
Laboratoire de Mécanique et d'Acoustique
4 Impasse Nikola Tesla, CS 40006 13453 Marseille Cedex 13, France

Philippe Herzog [3]
ARTEAC-LAB
29 rue Saint-Savournin, 13005 Marseille, France

Romain Boulandet [4]
HEPIA - Haute école du paysage, d'ingénierie et d'architecture
Rue de la Prairie 4, 1202 Genève, Suisse

ABSTRACT

An active device has been designed and built at LMA to control low-frequency reflections on the absorbing walls of a semi-anechoic room: the sound pressure reflected by the walls in the presence of an unknown source is estimated by linear filtering of the total sound pressure near the walls, then neutralized using acoustic sources placed on the walls. Here, we present 2D numerical simulations, involving monopole sources and series of damped analytic modes, which have enabled us to optimize the active device, in particular to (i) deal with resonance frequencies at which cancelling the diffracted pressure near the walls is not sufficient to cancel it inside the room, (ii) minimize the number of the total pressure measurement points required to estimate the pressure diffracted by the walls at each location, and (iii) select the strategy for minimizing the virtual signals corresponding to the diffracted pressure. Simulations show that with the optimized device, the control remains efficient up to frequencies corresponding to one wall source per wavelength and a little less than two pressure sensors per wavelength. Experiments are underway to compare measurements with simulations.

[1] friot@lma.cnrs-mrs.fr

[2] pinhede@lma.cnrs-mrs.fr

[3] philippe.herzog@arteac-lab.fr

[4] romain.boulandet@hesge.ch

1. INTRODUCTION

A strategy proposed for the active control of the field scattered by any surface in the presence of unknown acoustic sources [1, 2] can be applied to global control in anechoic rooms of the wall reflections that wall wedges fail to absorb at very low frequencies [3–8] (typically for wavelengths longer than 4 times the wedge length). A room has been built at LMA to demonstrate the validity of the concept in the case of a small semi-anechoic room. Numerical simulations are presented here to help specify the number and position of transducers to be placed in the room to implement the control.

After briefly recalling the theoretical basis of the control and presenting a 2D numerical model of the room in the frequency domain, we will consider three particular problems posed by the proposed device:

1. canceling the pressure scattered by the walls on a surface covering them guarantees the cancellation of this pressure inside the surface except at the resonance frequencies of the volume delimited by the surface [9]. The numerical simulations presented here effectively demonstrate the singularity of global control when using an array of microphones meshing a regular surface. It will be shown how some irregularity of the minimization surface may regularize the control in practice.

2. The control strategy studied here is based on estimating the pressure scattered by the walls at a set of minimizing points by means of appropriate linear filtering of the total pressure measured at a set of microphones. Several strategies for reducing the number of microphones to be used were compared, with a view to reducing control complexity for subsequent real-time implementation. In particular, we assessed whether, for the same number of estimation microphones, it would be preferable to select them close to the estimation point or to distribute them over all the walls.

3. The scattered pressure estimated at a point can be seen as the signal provided by a virtual microphone, and the strategy studied here is similar to the Remote-Microphone technique (RM) [10] in this context. Here we present the control results also obtained with the alternative Additional-Filter method (AF) [11] for control at virtual microphones.

2. CONTROL THEORY AND 2D MODELING OF AN ACTIVE SEMI-ANECHOIC ROOM

2.1. Overview of the control strategy

This section briefly summarizes the principles of the control strategy studied here, more details are given e.g. in [8].

Whatever the acoustic sources present, Green's representation of pressure p_{sca} scattered from a closed surface S is classically written, at point $\mathbf{r}$ and angular frequency ω, as a function of total pressure p over S :

$$p_{sca}(\mathbf{r},\omega) = \iint_S \left[G(\mathbf{r}|\mathbf{r}_0,\omega)\frac{\partial}{\partial n_0} p(\mathbf{r}_0,\omega) - p(\mathbf{r}_0,\omega)\frac{\partial}{\partial n_0} G(\mathbf{r}|\mathbf{r}_0,\omega) \right] dS_0 \tag{1}$$

where G is the acoustic Green's function for the propagation medium considered in the absence of the surface S. The active control strategy considered here is based on the estimation of the scattered pressure, with an adequate array of K ordinary pressure microphones, using a discrete approximation of the surface integral:

$$p_{sca}(\mathbf{r},\omega) \simeq \sum_{k=1}^{K} g_k(\mathbf{r}|\mathbf{r}_k,\omega)\, p(\mathbf{r}_k,\omega) \tag{2}$$

Coefficients g_k, combinations of an a priori unknown Green's function and generalized impedances, do not depend on the sources. They can be identified off-line, from measurements with known sources, and then used with unknown sources.

The microphones providing total pressure measurements for scattered pressure estimation can also be the points where the scattered pressure is estimated and minimized. If, in an anechoic room, these microphones cover all the walls, canceling the scattered pressure on this closed surface guarantees global control inside the surface except at the Dirichlet resonance frequencies of the volume bounded by the surface [9]. In the case of a semi-anechoic room, controlling with microphones in front of the walls and ceiling only, but not the floor, means controlling on the closed surface obtained by including the mirror images of the microphones with respect to the floor.

2.2. Construction and equipping of a semi-anechoic demonstration room

Figure 1 shows the room that was built at LMA for testing the control of low-frequency wall reflections. Loudspeakers are placed near the walls to cancel out the scattered field as close as possible to where it is generated. Off-the-shelf cheap loudspeakers were chosen for active control in the 100-400 Hz range. Specific sources would be needed to deal with the 20-100 Hz range in a full-scale anechoic room but they are not needed to demonstrate the control concepts. Aan array of microphones is positioned in front of the room walls. These microphones provide the total measured pressures needed to estimate the scattered pressure at each of these microphones, and these estimates will be used as the active control minimization signals.

Figure 1: The active set-up for controlling low-frequency wall reflections

Once the active low-frequency control system has been developed and validated, sound-absorbing materials will be inserted between the wall sources and the microphones. The intended result is a semi-anechoic room combining active and traditional passive absorption for higher frequencies. Similarly, in an existing anechoic room, a device for active control of very low-frequency reflections could be installed with acoustic sources in the plenum between the absorbing wedges and the walls, and an array of microphones positioned in the tips of the absorbing wedges. Note that an active system may reduce the size of the absorbing wegdes required for anechoicity in a given room.

2.3. 2D low-frequency modelling of the room without absorbing material

Several numerical models were developed and used prior to equipping the room to specify the number and position of transducers to be used. As the controllability of an acoustic field depends on parameters such as the number of transducers per wavelength or the distance between primary and secondary sources, the global visualizations of the acoustic field provided by a 2D model are particularly useful for dimensioning an active control system. Therefore only simple

2D simulations of the semi-anechoic room are presented here, full 3D Finite Element Modelling having been used only to confirm the relevance of the dimensioning rules deduced from the 2D simulations [12].

The 2D model used for the simulations below is a rectangular cavity $\mathscr{S}$ of dimensions $4.22 \times 2.77\,\mathrm{m}^2$, corresponding to the two smallest dimensions of the room built at LMA, whose third dimension is implicitely supposed infinite (it is 5.34 m at LMA). In this cavity the pressure radiated in $\boldsymbol{r}$ by a source in $\mathbf{r}_0$, considered as a linear monopole with surface flow q, can be approximated as a finite sum of damped normal modes:

$$p(\mathbf{r},\mathbf{r}_0) = \rho c^2 j\omega q \sum_{n=0}^{N} \frac{\boldsymbol{\psi}_n^t(\mathbf{r})\boldsymbol{\psi}_n(\mathbf{r}_0)}{(\omega_n^2 + 2j\xi_n\omega_n\omega - \omega^2)\int_{\mathscr{S}} \boldsymbol{\psi}_n^2 d\mathscr{S}} \tag{3}$$

where ρ designates the air density and c the sound speed. In the absence of absorbing material on the walls, the room is poorly damped, so the modes $\boldsymbol{\psi}_n$ and eigenfrequencies ω_n to be considered can be those of the rigid-edged cavity. The damping ratios ξ_n to be used in Equation 3 were obtained using Finite Element Modelling, in which a real surface impedance constant with frequency, uniform on the walls, high but not infinite except for the floor, corresponding to an absorption of 2% typical of plaster at very low frequencies, was taken as the boundary condition.

In 2D, the pressure radiated by a monopole in a free field can be written as :

$$p_{dir}(\mathbf{r},\mathbf{r}_0) = \rho j\omega q \frac{-i}{4} H_0^{(2)}(\frac{\omega}{c}\|\mathbf{r}-\mathbf{r}_0\|) \tag{4}$$

where $H_0^{(2)}$ is the zero-order Hankel function of the second kind. The pressure scattered by the walls of a semi-anechoic room containing a monopole can finally be written taking into account the image source at $\mathbf{r'}_0$ of the monopole with respect to the room floor:

$$p_{sca}(\mathbf{r},\mathbf{r}_0) = p(\mathbf{r},\mathbf{r}_0) - p_{dir}(\mathbf{r},\mathbf{r}_0) - p_{dir}(\mathbf{r},\mathbf{r'}_0) \tag{5}$$

The control simulations presented below are performed frequency by frequency, without taking into account the causality constraint imposed on real-time active control. At every frequency, optimal control is therefore obtained directly by pseudo-inversion of the frequency response matrix between the control sources and the minimizing microphones.

3. PRACTICAL REGULARIZATION OF BOUNDARY PRESSURE CONTROL

In this section, we focus on the controllability of wall-scattered sound pressure inside a semi-anechoic room measurement zone, using sources and microphones close to the room walls, assuming the scattered pressure can be measured directly. Controlling an acoustic sound field by controlling the pressure at an enclosing array of microphones is usually reffered to as Boundary Pressure Control (BPC) [9, 13].

Figure 2 shows two set-ups for 2D control simulations which differ only in the position of the 18 microphones placed close to the walls. 11 monopole sources are placed on the walls and ceiling of the semi-anechoic room. 352 points for calculating the pressure scattered by the walls are also considered to assess the effectiveness of global control in the room measurement zone.

Figure 3 shows as a function of frequency the Root-Mean-Square (RMS) value, without and with control, of the scattered pressure at 352 observation points in the measurement zone when the surface flow rate of the primary monopole placed in the room center is equal to 10^{-7} m^2/s. Calculations for this and subsequent figures were performed from 20 to 400 Hz in steps of 0.1 Hz, truncating the summation in Equation 3 the first 91 modes with resonance frequency below 500 Hz.

The uncontrolled scattered pressure is at a high level, with marked resonances. In the first instance, minimizing the scattered pressure at the 352 observation points with control sources

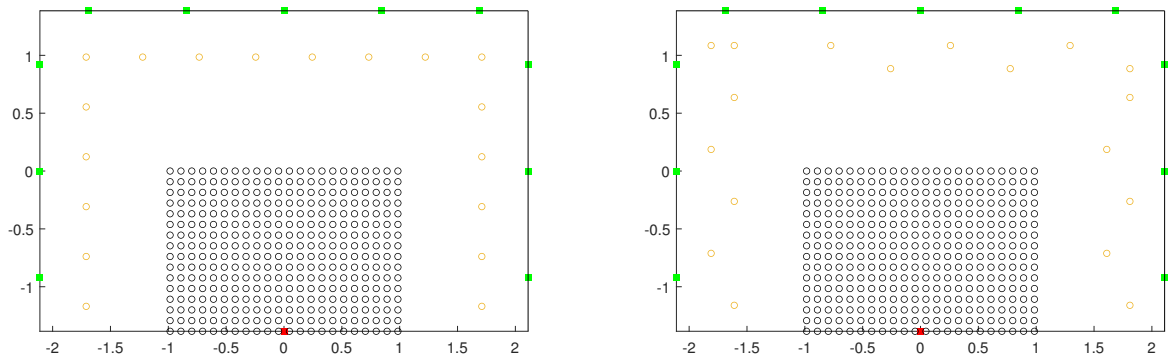

Figure 2: Two simulation set-ups for control of the acoustic pressure scattered by the walls of a semi-anechoic room: primary (monopole) source ■, control sources ■; scattered pressure sensors near the walls o and in the room measurement zone o.

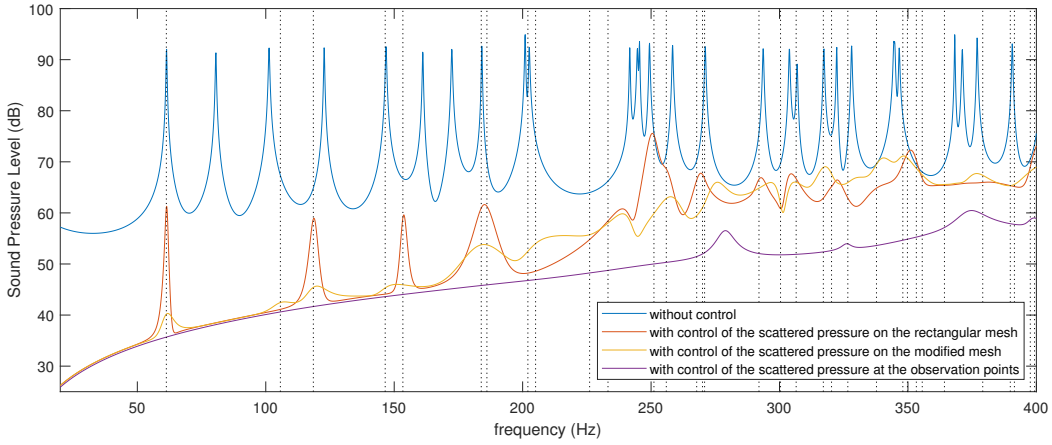

Figure 3: RMS of the scattered acoustic pressure in the room measurement zone with control of exact scattered pressure signals.

results in very high attenuation, not only at resonances. Further simulations showed that, below 250 Hz, the residual level of scattered pressure did not decrease with an increase in the number of sources, sufficient to control the simultaneously resonating modes. This residual scattered pressure results is only numerical noise at the output of the control computation. Above 250 Hz, however, the bumps in the residual pressure correspond to a slight loss of controllability with only 11 sources.

Secondly, by minimizing the scattered pressure at the 18 microphones arranged in three lines close to the walls, very good attenuation is also achieved on the 352 observation points up to 200 Hz, except around a few isolated frequencies. The vertical dotted lines in figure 3 mark the Dirichlet resonance frequencies of the rectangle supporting the microphones and their image relative to the floor. It is indeed around some of these frequencies that control on the regular mesh of wall microphones does not induce very good control inside the room, as might be expected with BPC [9].

By introducing some disorder into the position of the microphones in the wall, as shown in figure 2 on the right, we can see that the theoretical singularity of global control has much less influence on its performance in practice. One possible explanation is that out of alignment microphones pick up some information on the normal pressure gradient, with the simultaneous

cancellation of pressure and normal gradient on a closed surface guaranteeing cancellation inside, without any singular frequencies.

Finally, beyond 200 Hz, pressure control on the wall microphones is worth up to 400 Hz but it leads to much less effective control at the center of the room than that obtained by directly controlling pressure on the observation points. The number of microphones is no longer sufficient for global control. With around 0.5 m between microphones, the frequency zone from which control is no longer global corresponds to a mesh of the order of 2 microphones per wavelength, which is quite usual in acoustic field sampling, with about one secondary source per wavelength.

4. CONTROL OF SCATTERED PRESSURE ESTIMATES

4.1. Estimation of the scattered pressure using all the microphones

The control strategy studied here relies, as indicated by Equation 2, on estimating the scattered pressure at minimization points by linear filtering of the total pressure measured at several points. As the operator in Equation 1 mapping the total pressure to the scattered pressure close to the walls does not depend on the acoustic sources, the coefficients g_k in Equation 2 can be identified by placing at several places a reference source [14], of known radiation in free field, allowing the simultaneous collection at several points of the total pressure and the pressure scattered by the walls. If $\mathbf{P}(\omega)$ and $\mathbf{P}_{sca}(\omega)$ denote matrices each column of which is respectively the vector of total and scattered pressures measured at angular frequency ω, then we can search for the matrix $\mathbf{G}(\omega)$ that minimizes the Frobenius norm :

$$J = \|\mathbf{P}_{sca}(\omega) - \mathbf{G}(\omega)\mathbf{P}(\omega)\|_{Fro}^2 \tag{6}$$

The solution to this inverse problem, possibly regularized if the number of reference source positions used is smaller than the number of measurement points, is a square matrix of dimension this number of measurement points. In practice, $\mathbf{G}(\omega)$ is easily obtained by pseudo-inversion of the matrix $\mathbf{P}(\omega)$.

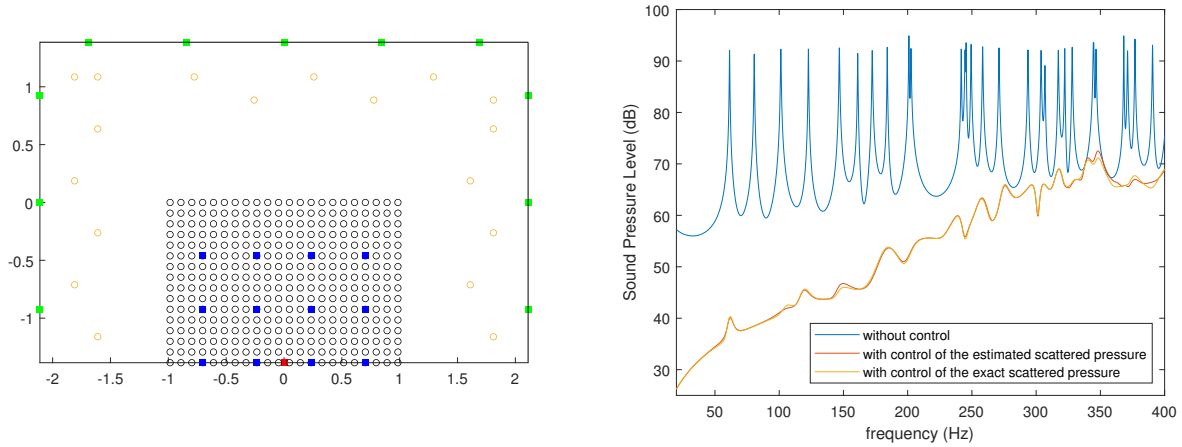

Figure 4: Set-up for the estimation of the scattered pressure and RMS of the scattered acoustic pressure in the room measurement zone with control of exact and estimated scattered pressure signals.

Figure 4 shows an active semi-anechoic room configuration for 2D simulation of the control of the wall scattered pressure estimated via total pressure filtering. A reference monopole is placed at 12 positions towards the center of the room to generate the data needed to calculate at every frequency the 18×18 matrix $\mathbf{G}$ which maps the total pressure at all the microphones to the estimated scattered pressure at all the microphones. Figure 4 also shows the performance of the control when the *exact* scattered pressure or the *estimated* scattered pressure is minimized

with a primary source placed at a different position from those taken by the reference source. The performance of the two controls is very similar, the estimation of the scattered pressure from the 18 total pressure measurements is very good.

4.2. Estimation of the scattered pressure using selected microphones

In order to reduce the complexity of a future real-time control system, it may be advantageous to use only some of the microphones to estimate the pressure scattered at one given point. Two options are to select either the microphones closest to the point of estimation or microphones at regular intervals, starting from the point of estimation. In the first case, matrix **G** in Equation 6 must be a band matrix, and in the second case a matrix whose diagonals are either full or zero. From a numerical point of view, a simple way to obtain solution matrices of Equation 6 with this type of constraint is to transform the equation whose unknown is a matrix into an equation whose unknown is a vector, which is easily written using the vectorization operator vec and the Kronecker product $\otimes$:

$$J(\omega) = \|\mathbf{P}_{sca} - \mathbf{GP}\|_{Fro}^2 = \|\mathrm{vec}(\mathbf{P}_{sca} - \mathbf{GP})\|_2^2 = \|\mathrm{vec}(\mathbf{P}_{sca}) - (\mathbf{P}^t \otimes \mathbf{I}_m)\mathrm{vec}(\mathbf{G})\|_2^2 \tag{7}$$

where $\mathbf{I}_m$ is the identity matrix of dimension the total number of microphones. The rows of this equation corresponding to zero coefficients in **G** can be removed and the non-zero components of the vector vec(**G**) are obtained by pseudo-inversion of the remaining linear system. Matrix **G** is then easily reconstructed by combining these components and the null coefficients.

Figure 5 compares the control performance obtained by estimating the scattered pressure on each of the 18 minimization microphones using the total pressure either:

- on all the 18 microphones,
- on the microphone where we want to estimate the scattered pressure and the 3 neighboring microphones on either side,
- on the microphone where we want to estimate the scattered pressure and one microphone out of 5 on either side.

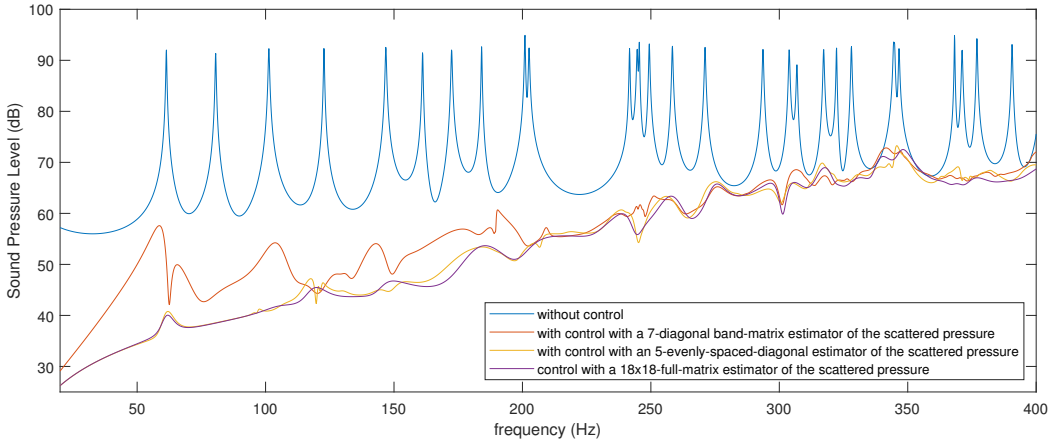

Figure 5: RMS of the scattered acoustic pressure in the room measurement zone with control of various estimations of scattered pressure signals.

In the first case, **G** is a full matrix with 324 coefficients and one scattered pressure is estimated from 18 signals. In the second case **G** is a band matrix with 114 non-zero coefficients and one scattered pressure is estimated from 4 to 7 signals, depending on the position of the estimation

point. In the third case **G** is a sparse matrix with 82 non-zero coefficients and one scattered pressure is estimated from from 4 or 5 total pressure signals. Although fewer signals are used in the third case than in the second, estimating the scattered pressure with microphones on all the walls gives better results, particularly at very low frequencies, than estimating it with microphones close to the estimation points. This result may seem counter-intuitive but it is easily explained by the multiple reflections taking places: a wall reflects wavefronts that do not come directly from an acoustic source, but are already the result of previous reflections on other walls.

In conlusion, few measurement points can be used to accurately estimate the scattered pressure at every point close to the walls, provided that measurements are taken on all the walls and not only around the estimation point; scattering from the walls is a global phenomenon.

5. ADDITIONAL-FILTER VS. REMOTE-MICROPHONE TECHNIQUE

The linear filtering of total pressure signals to obtain an estimate of a scattered pressure signal is analogous to the so-called Remote-Microphone technique for estimation of noise at virtual microphones [10]. A more recently introduced approach to this control on virtual microphones consists in filtering not the signals on the real microphones, in order to generate minimization signals, but rather the control signals to be provided to minimize these signal on the real microphones, in order to generate the control signals that minimize the signal at the virtual microphones. This so-called Additional Filter method has led in some cases to better results than the Remote-Microphone technique [10]. It could be of interest in the case of the semi-anechoic room under study, because the number of sources is smaller than the number of microphones. The matrix to be identified at each frequency is therefore smaller with the AF, and could be obtained from data collected with a smaller number of reference source positions. As moving this heavy reference source around the room is by far the most tedious step in the whole control strategy studied here, we wanted to compare the RM and AF in 2D simulations of the semi-anechoic room.

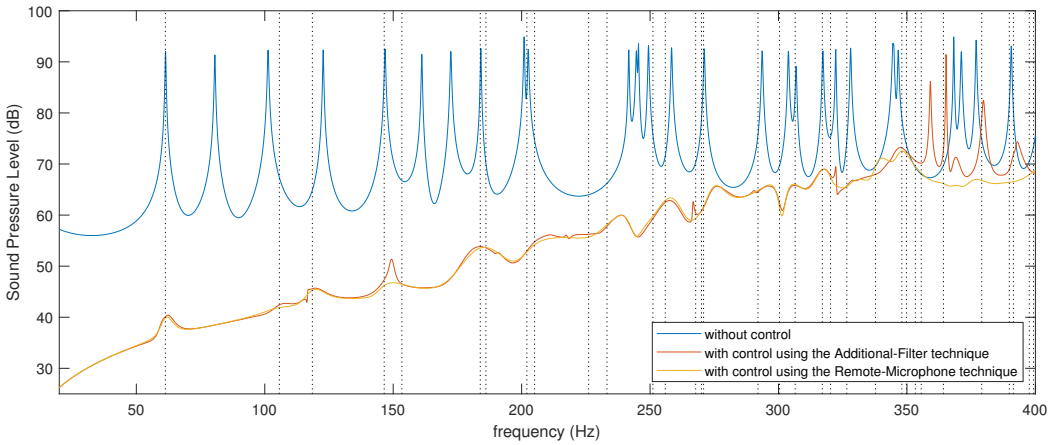

Figure 6: RMS of the scattered acoustic pressure in the room measurement zone with control using the Remote-Microphone or the Additional-Filter technique.

Figure 6 shows the control simulation results obtained with each of the two methods when all the wall microphones are used for scattered field estimation with the device shown on the right of Figure 4. At low frequencies, the AF technique leads to control results similar to those obtained with the RM technique, except at a few frequencies where the residual scattered pressure shows a small peak. These frequencies are close to the singular frequencies, marked by the vertical dotted lines, of the Boundary Pressure Control device shown on the left of the Figure 4. It is likely that control which is more difficult to achieve at these frequencies, leads to a

poorer estimation of the operator switching from "total" to "scattered" when considering optimal control signals rather than pressure signals. Beyond 350 Hz, the results of the AF technique are no longer acceptable. At these frequencies, the density of secondary sources no longer allows global control of the scattered pressure in the room, the control signals only allow local minimization on the microphones, and the Additional-Filter naturally no longer accounts for the underlying continuous operator enabling the mapping from real to scattered signals.

From a practical point of view, it was decided, in the light of this simulation and others carried out by varying the number of positions of the reference source, to stick to the Remote-Microphone Technique for experiments carried out in the room built at the LMA.

6. CONCLUSIONS

The simulations presented have led to a number of practical results which have been directly taken into account in equipping the active semi-anechoic room built at the LMA:

1. microphone meshing of an irregular minimization surface is sufficient in practice to overcome the theoretical singularity of Boundary Pressure Control at the resonant frequencies of the volume bounded by the surface.

2. The estimation from total pressure measurements of the scattered pressure at one location is, for comparable numbers of measurement points, much better when these points cover the whole diffracting surface rather than the vicinity of the estimation point. Scattering from a surface is a global phenomenon.

3. In the case of the semi-anechoic room device considered here, control of the scattered pressure using Remote Microphone technique gives more reliable results than the Additional Filter method.

Experimental tests have begun in the room built at LMA, and the results will be presented at a later date.

REFERENCES

1. E. Friot and C. Bordier. Real-time active suppression of scattered acoustic radiation. *Journal of Sound and Vibration*, 278(3):563–580, 2004.
2. E. Friot, R. Guillermin, and M. Winninger. Active control of scattered acoustic radiation: A real-time implementation for a three-dimensional object. *Acta Acustica united with Acustica*, 92:278–288, 2006.
3. E Friot. Control of low-frequency wall reflections in an anechoic room. In *Active 2006*, Adelaide, 2006.
4. E. Friot and A. Gintz. Estimation and global control of noise reflections. In *Active 2009*, Ottawa, 2009.
5. D. Habault, E. Friot, P. Herzog, and C. Pinhede. Active control in an anechoic room : Theory and first simulations. *Acta Acustica united with Acustica*, 103(3):369–378, 2017.
6. C. Pinhède, D. Habault, E. Friot, and P. Herzog. Active Control of the Diffracted Field by the Reflecting Wall of a Semi-Anechoic Room. In *Forum Acusticum 2020*, Lyon, 2020.
7. C. Pinhède, D. Habault, E. Friot, and P. Herzog. Active control of the field scattered by the rigid wall of a semi-anechoic room—Simulations and full-scale off-line experiment. *Journal of Sound and Vibration*, 506:116–134, 2021.
8. C. Pinhède, R. Boulandet, E. Friot, M. R. Allado, R. Côte, and P. Herzog. Towards an active semi-anechoic room: Simulations and first measurements. In *Forum Acusticum 2023*, Torino, Italy, 2023.

9. N. Epain and E. Friot. Active control of sound inside a sphere via control of the acoustic pressure at the boundary surface. *Journal of Sound and Vibration*, 299(3):587–604, 2007.
10. A. Roure and A. Albarrarazin. The Remote Microphone Technique for Active Noise Control. In *INTER-NOISE and NOISE-CON 1999*, volume 5, pages 1233–1244, Fort Lauderdale, 1999.
11. J. Zhang, S. J. Elliott, and J. Cheer. Robust performance of virtual sensing methods for active noise control. *Mechanical Systems and Signal Processing*, 152:107453, 2021.
12. R. Boulandet, M. Allado, C. Pinhède, E. Friot, R. Côte, and P. Herzog. Simulation of a hybrid (passive/active) acoustic measurement room. In *COMSOL 2023 Conference*, Munich, Germany, 2023.
13. S Takane, Y Suzuki, and T Sone. A New Method for Global Sound Field Reproduction Based on Kirchhoff's Integral Equation. *ACUSTICA*, 85:250–257, 1999.
14. C. Pinhède and P. Herzog. Design and measurement of a reference source at lower frequencies. In *Forum Acusticum 2020*, Lyon, 2020.